**Systematic Quantitation of Histologic Patterns Shows Accuracy in Reflecting Cirrhotic Remodeling**

**Running title:** Quantitating dynamic histologic cirrhosis

Yan Wang[1,2], Wei Huang[3], Ruhua Li[2], Zhaoqiang Yun[3], Youfu Zhu[1], Jinlian Yang[2], Hailin Liu[4], Zhipeng Liu[4], Qianjin Feng[3], Jinlin Hou[1].

[1]State Key Laboratory of Organ Failure Research, Guangdong Provincial Key Laboratory of Viral Hepatitis Research; Department of Infectious Diseases and Hepatology Unit, Nanfang Hospital, Southern Medical University, Guangzhou, China.

[2]Biomedical Research Center, Southern Medical University, Guangzhou, China.

[3]School of Biomedical Engineering, Southern Medical University, Guangzhou, China.

[4]School of Clinical Medicine, Zhujiang Hospital, Southern Medical University, Guangzhou, China.

**Contact information**

Prof. Yan Wang MD, PhD

Biomedical Research Center, Southern Medical University

No1023 Sha Tai Nan Avenue, Guangzhou 510515, China

Tel +8620 6164 7396; Email yanwang@smu.edu.cn.

And

Prof. Qianjin Feng PhD

School of Biomedical Engineering, Southern Medical University

No1023 Sha Tai Nan Avenue, Guangzhou 510515, China

Tel +8620 6164 8286; Email qianjinfeng08@gmail.com.

**Authorship statement**

Guarantor of the article: Yan Wang.

YW designed the project and drafted the manuscript. YW and QJF conceived the algorithm and supervised the study. WH, ZQY, and QJF created the algorithm. HLL and ZPL collected experimental data. YFZ and YW collected clinical data. WH, RHL, JLY, and HLL collected image data. WH, RHL, and YW analyzed and interpreted the data. JLH supervised the study and critically revised the manuscript.

All authors approved the final version of the manuscript and the authorship list.

**Disclosure statement**

All authors have no conflicts of interest with respect to the manuscript.

**ABSTRACT**

*Background and Aim*

There still lacks a tool for precisely evaluating cirrhotic remodeling. Histologic distortion characterized in cirrhosis (i.e. cirrhotic patterns) has a validated pathophysiological meaning and the potential relevance to clinical complications. We aimed to establish a new tool for quantify the cirrhotic patterns and test it for reflecting the cirrhotic remodeling.

*Methods*

We designed a computerized algorithm (*q*CP) dedicated for the analysis of liver images acquired by second harmonic microscopy. We evaluated its measurement by using a cohort of 95 biopsies (Ishak staging F4/5/6=33/35/27) of chronic hepatitis B (CHB) and a carbon tetrachloride-intoxicated rat model for simulating the bidirectional cirrhotic change.

*Results*

*Q*CP can characterize 14 histologic cirrhosis parameters (HCPs) involving the nodules, septa, sinusoid and vessels. For CHB biopsies, the mean overall intra- and inter-observer agreement was 0.94±0.08 and 0.93±0.09, respectively. The robustness in resisting sample adequacy-related scoring error was demonstrated. The proportionate areas of total (CPA), septal (SPA), sinusoidal, and vessel collagen, nodule area, and nodule density (ND) were associated with Ishak staging ($p<0.01$ for all). But only ND and SPA were independently associated ($p\leq0.001$ for both). A HCPs-composed *q*CP-index demonstrated an excellent accuracy in quantitatively diagnosing evolving cirrhosis (areas under receiver operating

characteristic curves 0.95-0.92; sensitivity 0.93-0.82; specificity 0.94-0.85). In the rat model, changes in CPA, SPA, and ND had strong correlations with both cirrhosis progression and regression and faithfully characterized the histologic evolution.

*Conclusions*

*Q*CP preliminarily demonstrates potential for quantitating cirrhotic remodeling with high resolution and accuracy. Further validation with in-study cohorts and multiple-etiologies is warranted.

**Keywords**

Liver cirrhosis; liver fibrosis; fibrosis change; biopsy; quantitative image analysis; chronic hepatitis B; animal model.

## INTRODUCTION

Cirrhosis is a leading cause of liver related mortality [1]. Historically, cirrhosis has been considered to be irreversible. However, recent studies of hepatitis B viral suppression and hepatitis C cure have raised the possibility of regression of cirrhosis [2, 3]. Additionally, multiple therapies targeting advanced fibrosis are being developed with the goal of reversing cirrhosis [4]. A major limiting factor in such development is the historical view of cirrhosis as a single histological entity. It is well established that the dynamic range of fibrosis progression extends from bridging fibrosis to cirrhosis in viral hepatitis and led to the extended Ishak fibrosis scoring system [5]. However, this does not capture the ongoing fibrotic remodeling of the liver

that goes on even when cirrhosis (Ishak F6) is fully established. There is currently no well validated method to capture bidirectional remodeling of fibrosis in the context of viral hepatitis and advanced hepatic fibrosis.

Cirrhosis is characterized by a diffuse histologic distortion [6], i.e. the cirrhotic patterns, of which the septal width, nodule size and total fibrosis area have been frequently verified to be associated with major endpoints [7-12]. However, among all the cirrhotic patterns, collagen area (or content), defined as the area ratio of collagen to tissue-section, is the only one that is analyzed based on the fully-quantitative measurement and meanwhile, that has been most intensively investigated in clinical studies [12-15]. Given that cirrhotic patterns associated with clinical events are indeed not limited to the one of collagen area [7-12], the prevalent application of collagen area suggests that a fully-quantitative measurement may technically benefit an extensive assessment and thus, provide the precise data of histologic change in cirrhosis, which could be helpful to address the clinical needs.

For quantitating fibrosis patterns, based on the second harmonic generation (SHG) microscopy [16], we previously developed a *q*Fibrosis algorithm which measures the texture features of collagen fiber for assessment [17]. However, the cirrhotic patterns, such as the presence of nodules and annular septal bands and their geometrical features, are beyond the scale of morphologic targets identifiable in *q*Fibrosis algorithm. Nevertheless, such items are what the clinicians may have more interest to know about for the overall assessment of fibrotic remodeling [7-9, 18, 19]. Therefore, in present study, we first developed an automated algorithm for systematically quantitating the cirrhotic patterns based on a new strategy of

image-analysis; and then we evaluated its accuracy in characterizing the cirrhotic remodeling.

## MATERIALS AND METHODS

### Rat model of cirrhosis progression and regression

As previously described [20], adult male Sprague Dawley rats (200-250g) were treated with carbon-tetrachloride ($CCl_4$) at 0.15-0.2 mL/100 g, ip, twice weekly for 12 weeks, and then underwent spontaneous recovery for another 12 weeks. Liver specimens (n=4-5 for each time point) from the left lateral lobe were harvested at 6, 8 and 12 weeks of $CCl_4$ treatment and at 2, 4 and 8 weeks after cessation of intoxication. The tissue samples were routinely processed. Sample slides (4 μm thickness) were stained with Masson trichrome and evaluated using the Ishak fibrosis staging system [5] by a pathologist in Department of Pathology, Guangzhou Huayin Medical Laboratory Center (Guangzhou, China). For second harmonic generation (SHG) imaging, the sample slides underwent microscopy without staining. Serum samples were isolated at the time of liver harvesting and stored at -80˚C until analysis of hepatic biochemical profiles (AEROSET system, Abbott Laboratories, USA). All the above animal work was previewed and approved by the Animal Care and Use Committee of Southern Medical University.

**Clinical liver biopsy samples**

Clinical samples were collected from the stored biopsy blocks of chronic hepatitis B (CHB) patients referral to the Department of Infectious Diseases at Nanfang Hospital (Guangzhou, China) for medical examination or treatment between 2005 and 2013. All the patients had given written informed consent for biopsy and permission for use of their medical records. The study was conducted according to the Declaration of Helsinki guidelines and was approved by the Ethics Committee of Nanfang Hospital. The inclusion criteria were: treatment naïve biopsy, histological diagnosis of advanced fibrosis or cirrhosis, sample length ≥10 mm and without over-fragmentation (i.e., if fragmented, all fragments ≥3 mm). Exclusion criteria were: diagnosis of other etiologies of liver diseases, concomitance of fatty liver disease or chronic venous outflow obstruction, and co-infection with hepatitis C, D or human immunodeficiency virus. The specimens were routinely processed. Masson trichrome-stained samples (4 μm thickness) were evaluated using the Ishak fibrosis staging [5] by a blinded senior liver pathologist (YFZ) in the hospital department. For SHG imaging, the slices were prepared in the same way as for the rats. Overall, 95 core needle biopsies were included. The mean length was 20.0 ± 7.8 mm (10.0-50.0 mm) with 0-7 fragments. The number of complete portal triads was 11 ± 4 (4-31). The biopsy numbers were evenly distributed between Ishak F4 (33), F5 (35), and F6 (27).

**SHG image acquisition**

An SHG/two-photon excitation fluorescence microscope (Genesis, HistoIndex Singapore) was employed for detecting fibrillar collagen as described previously [17]. The technical principle is that the endogenous signals of fibrous collagen and tissue parenchyma can be sensitively and specifically identified by nonlinear optical imaging with second harmonic generation and two-photon excitation fluorescence microscopy, respectively [16]. Briefly, liver tissue slices (4 μm thickness) were routinely processed without specific staining. Then for each sample, the slice was imaged with a 20 × objective and 512 × 512 pixels of resolution. Three images of 13 × 13 multi-tiles were randomly acquired for a final size of 4.84 $mm^2$ in each animal specimen; for each clinical biopsy, the whole section was imaged. All images were processed using the *q*CP algorithm developed in the present study.

**Establishing a computerized image-analysis algorithm for quantitating the cirrhotic patterns**

Details for the design and calculation of the algorithm named *q*CP are described in the **Supplementary Materials**. Briefly, a procedure of multi-channel image-processing was developed to label and digitally segment the image-patterns of the principle cirrhotic patterns, involving the nodules, septal bands, vessels and sinusoid. Each geometrical parameter of the cirrhotic pattern was then measured as a feature element of the histological cirrhosis parameters (HCPs). The process of image-analysis by *q*CP is illustrated in **Fig.1**. Result of image-procession is represented by **Fig.S1**.

**Building a *q*CP-index model for simulating a dichotomized decision**

The HCPs were then included to develop the function model, namely *q*CP-index for exploring the potential application. A soft-max logistic regression model [21] was taken as an inducer of multi-category classifier. With the algorithm of stratified ten-fold cross-validation [22], HCP datasets of the 95 biopsies were used for training and testing the inducer to select the classifier, *q*CP-index. Detailed calculation is described in the **Supplementary Materials.**

**Statistical analysis**

Analyses were performed using SPSS version19.0 (IBM Corporation, USA) or MATLAB® 2012a (MathWorks Inc., USA). Spearman's correlation was used to assess the relationship between variables. Intra and inter -observer agreement was evaluated by intraclass correlation coefficient (ICC) analysis. Multivariable logistic analysis was used to test the independent association of continuous variables with ordinal data. The area under the receiver-operating characteristic curve (AUC) was used for performance analysis. Two-sided p values $<0.05$ were considered significant.

## RESULTS

### Quantitation of histological cirrhotic patterns by *q*CP

*Q*CP, a new automated algorithm of image-analysis was developed dedicated for quantitating the cirrhotic patterns (**Supplementary Materials** and **Fig. 1**). A total set of 14 HCPs were identified and measured as continuous variables relative to their original dimensions. The HCPs encompassed the geometrical features of blood vessels, including the vascular area (VA), vascular perimeter (VP), vascular long-axis length (VLL), vascular short-axis length (VSL), vascular thickness (VT), and vascular density (VD); the proportions of collagen areas in different sublobules, including the total collagen proportionate area (CPA), vessel collagen proportionate area (VPA), septal collagen proportionate area (SPA), and perisinusoidal collagen proportionate area (FPA); and the geometrical features of nodules, including the nodule area (NA), nodule long-axis length (NLL), nodule short-axis length (NSL), and nodule density (ND). Definitions of all the HCPs are described in **Table S1** and are illustrated in **Fig. S1**.

### Validation of clinical feasibility with CHB liver biopsies

We took Ishak fibrosis staging [5] as the standard reference for analyses, based on the following considerations. First, Ishak fibrosis staging [5] is among the most commonly used histological references in the studies of morphometric analysis [13-15, 23-25] and is widely recognized in clinical practice [26, 27], especially for the patients with chronic viral hepatitis. Second, given that aim of our study is to develop a tool for quantitating dynamic cirrhotic patterns, Ishak F4-6, representing the trend from bridging fibrosis to complete cirrhosis, can

suffice the need for showing the early cirrhotic evolution.

***Assessment of the methodological reproducibility***

We first determined whether the established procedure could have an acceptable reproducibility for assessing the clinical biopsies. Nine biopsies (three for each stage) were randomly selected from the included samples by an investigator (RHL). Image acquisition was independently performed by another two investigators (JLY and HLL), respectively; and was repeated a week later. All the images were analyzed using *q*CP by the fourth investigator (WH) blinded to the imaging-operators and clinical data of these samples. Data by *q*CP assessment were taken for the ICC analysis of all HCPs (**Table S2**). The overall intra- and inter-observer agreement was 0.94 ± 0.08 and 0.93 ± 0.09, respectively.

Then we evaluated the impact of sample adequacy on *q*CP assessment. We found that the length of liver biopsies had no impact on the Ishak score ($r_s$=0.03; p=0.79) and the HCPs such as CPA ($r_s$= -0.12; p=0.25), SPA ($r_s$= -0.04; p=0.71) and ND ($r_s$= -0.03; p=0.79). We then virtually reduced the samples' size by 50%. Relative to measurement of the original sizes, concordance by ICC analysis of the CPA, SPA, and ND measures were 0.89, 0.88, and 0.90, respectively. All data indicate that *q*CP measurement could have good resistance to the sample adequacy-related scoring issues.

***Correlation between HCPs and histological fibrosis stages***

We then measured HCPs across the Ishak stages (**Fig. 2** and **Table S3**). From F4-6, the HCPs such as VD, CPA, SPA, FPA and VPA kept increasing, meanwhile the nodules became smaller and more intense ($p<0.05$ for all) (**Fig. 3A**). ND ($r_s$=0.87), SPA ($r_s$=0.84) and CPA ($r_s$=0.83) demonstrated strong strength of correlation ($p<0.001$ for all) (**Table 1**). The characteristics of them at different stages are shown in **Fig. 4A**-**C**. In univariable analysis, HCPs such as CPA, SPA, FPA, VPA, VD, NA and ND were associated with Ishak stage ($p<0.05$ for all) (**Table S4**). In multivariable regression, only ND ($p<0.001$) and/or SPA ($p=0.001$) were independently associated (**Tables S5** and **S6**). Additional analysis by AUC shows that the combination of SPA and ND could have better performance to predict the fibrotic severity than the rest individual HCPs (**Fig. 5A**-**C** and **Table S7**).

***Performance of qCP-index in diagnosis of cirrhosis***

Given that in real practice, there is often a requirement for dichotomous decision, we developed a *q*CP-index to exemplify the application. The development process is illustrated in **Fig.1**. Data show that, compared with the index-model built with the 8 HCPs significantly correlated with Ishak scoring, the model incorporating all the 14 HCPs had a higher AUC (0.95 *vs.* 0.91) for discriminating F4 from F5,6 and a comparable AUC (0.92 *vs.* 0.91) for differentiating F5 and F6. Furthermore, by ten-fold cross-validation, accuracy rates of classification by the models with the 14 and the 8 HCPs were 84.3% and 80.1%, respectively. Thus, the model with all the 14 HCPs was eventually taken as *q*CP-index. Characteristics of the *q*CP-index measurement are shown in **Table 2** and **Fig. 4D**. An excellent diagnostic performance of *q*CP-index was verified in discriminating Ishak stages (AUC 0.95-0.92;

sensitivity 0.93-0.82; specificity 0.94-0.85) (**Fig. 5D**-**F** and **Table S7**), which is better than that of *q*Fibrosis (AUC 0.73) [17], implying the strength of the present study. Furthermore, the results might also suggest the potential application of all the 14 HCPs rather than a few of them for various clinical settings in the future studies.

**Validation of bidirectional cirrhosis in dynamic animal model**

***Correlation between the HCPs and change in the fibrotic severity***

In the $CCl_4$-induced bidirectional cirrhotic model [20], we first determined the changes of HCPs and liver biochemical function parameters across Ishak stages. From F4-6, the median CPA and SPA increased from 4.4% to 12.4% (p=0.001) and 3.5% to 11.0% (p=0.001), respectively; meanwhile the NA reduced by over 5-fold (p=0.004) and ND increased by 3.5-fold (p=0.002) (**Fig. 3B**). Changes in the hepatic biochemical function parameters demonstrated a pattern of worsening hepatic function, as expected (**Table S8**). The correlation to Ishak stages is shown in **Table S9**. Among all HCPs, the strong correlates in order of strength were ND ($r_s$=0.95; p<0.001), SPA ($r_s$=0.91; p<0.001), and CPA ($r_s$=0.89; p<0.001). By univariable logistic regression, CPA was associated with Ishak staging (p=0.048) (**Table S10**).

***Correlation between the HCPs and the injury course, hepatic biochemical function, and ascites***

With disease progression, NA ($r_s$= -0.85; p=0.008), ND ($r_s$=0.85; p=0.008), CPA ($r_s$=0.78; p=0.02) and SPA ($r_s$=0.76; p=0.03) had a strong correlation with the course of injury (**Table S11**). Among them, CPA, SPA and ND were closely associated ($|\beta|$> 0.5, p<0.05 for all) with 86% (6/7) to 71% (5/7) of the hepatic biochemical function parameters that were statistically

associated with fibrosis staging (**Table S12**). Ascites is a representative manifestation of decompensated cirrhosis. In $CCl_4$-induced cirrhotic rats, ascites can develop with progression of intoxication [28]. In this study, the diagnosis of ascites was defined as accumulation of fluid in the peritoneal cavity without blood or obvious infection, which was observed both in physical examination and operation of liver resection of the animal. ND ($r_s$=0.57; p=0.03) and SPA ($r_s$=0.55; p=0.04) were moderately correlated to the ascites development (**Table S13**). These results collectively indicate the pathophysiological relevance of HCPs, such as the CPA, SPA and ND, with cirrhosis development in the rat model.

***Cirrhosis regression versus progression***

The cirrhotic animal model had two opposite phases in its disease course and had to experience the same cirrhotic stage at the initial point of spontaneous recovery after 12 weeks of intoxication. Therefore, we explored whether there was any difference in the HCPs between the opposite evolving processes. Compared with the progression phase, median VA, VT, CPA, SPA, VPA, ND and NLL were significantly decreased over the course of recovery ($p<0.05$ for all), indicating their active remodeling in the initial phase of regression. However, there was no significant change in the NA across the two phases (p=0.07), which might imply the relatively belated recovery in the annular organization. Because the recovery was also verified by the concurrent improvement in the hepatic biochemical function parameters (**Table S14**), all data indicate that HCPs were sensitive to the histological changes associated with cirrhosis reversal, even if the cirrhotic state remained.

## DISCUSSION

In this study, we developed *q*CP, an algorithm of image analysis to systematically quantitate the cirrhotic patterns with documented pathophysiological relevance; data by evaluation with both the clinical biopsies and dynamic animal model show that *q*CP measurement can reflect the histologic changes in cirrhosis with high resolution and accuracy.

Cirrhotic patterns have been indicated of their relevance for many years. Our study shows the first instance of systematically quantitating them by using a computerized image-analysis algorithm, *q*CP particularly designed to address the need for identifying the overall morphology and geometric parameters of the histological cirrhotic patterns. Assessment data on using *q*CP show the merits. To test *q*CP's feasibility for clinical samples, we recruited biopsies from patients with CHB, a major local liver disease. Data show an excellent reproducibility of the *q*CP assessment. Interestingly, in further assessment, SPA and ND demonstrated more robustness than CPA alone for characterizing the histologic changes in advanced fibrosis stages. Because the CPA in our study was calculated based on the same definition as the documented[12, 13], SPA and ND could be considered as the representative HCPs in future studies of CHB-related cirrhosis. This result replicates previous reports [8, 9, 13, 18] but with more solid supporting data of measurement.

Correlation of CPA to Ishak staging in discriminating Ishak F4-6 have been investigated in hepatitis C or B patients in previous studies [13, 29]. However, in these studies, the SPA and ND variables were never included, and the values of CPA were not exactly the same as those in our study although the trend of CPA change is similar. Here, it is worthy to note that direct

comparison of the exact values of CPA or other variables between the independent studies is difficult, because the involved imaging technologies [13, 29], parameter definitions [29], or etiologies [30] often differ between the studies.

To further validate *q*CP algorithm for detecting bidirectional cirrhotic changes, we employed a well-recognized animal model [20] that is qualified for an intensive observation of the fibrotic remodeling, which however, is hard to perform in clinical settings. Data show that, as the intoxication persisted, total and septal collagen areas increased, and smaller nodules developed. These changes are consistent with the patterns of progressive cirrhosis as described [20]. Notably, ND appeared to be the variable statistically most correlated with fibrotic severity, which properly reflects the micronodular morphology represented by this model [20]. Cirrhosis regression is often associated with a net decrease in fibrosis content and the obviously thinning septal bands [19, 20]. This was reflected by a significant decrease in CPA and SPA as well as a significant reduction in vascular thickness and area, indicating the decaying fibrous bridge between the vessels. Meanwhile, nodular organization can persist during cirrhosis regression irrespective of the above decrease [19, 20]. Interestingly, this was also reflected in the analysis of HCPs by showing an insignificant change in NA across the whole landscape. Collectively, these animal data suggest that *q*CP algorithm could accurately reflect the meaningful histologic changes in cirrhosis remodeling.

Altogether, addressing the need for assessing histologic changes in cirrhosis, our study has the strength of a novel strategy for measuring cirrhotic patterns, a dedicated technical establishment, and a systematic validation in both experimental model and clinical biopsies. Besides, because of its validated relevance to Ishak staging, *q*CP could be used as a complement to Ishak staging for extra measuring of the changes in cirrhosis. All these make the present work distinct from other recently studies using SHG technology to detect liver fibrosis for various applications [17, 31-34]. Meanwhile, some issues also need to note in this study. First, *q*CP is a tool of fibrosis assessment using liver biopsy. Therefore, the inherent shortcomings of biopsy examination will barrier the performance of *q*CP assessment. Second, the clinical validation was based on CHB biopsies only. CHB remains a leading cause for liver cirrhosis and hepatocellular carcinoma (HCC) worldwide [35]. Fibrotic burden could be the most important risk factor for HCC development in CHB patients even with sufficient virologic remission [36, 37]. Therefore, CHB-related cirrhosis is an important topic. The other major liver diseases such as steatohepatitis have different patterns and courses in histology of fibrotic changes [38], whether *q*CP can work well in measuring the cirrhotic patterns with other etiologies needs additional separate data. Third, the present study did not additionally compare *q*CP with the other advanced histological systems such as the Laennec system [7] to categorize the intra-stages of cirrhosis. Indeed, the design of *q*CP has incorporated the cirrhotic patterns documented in these [7-9] and some other [6, 19, 20, 27] seminal studies. With the first stage of establishment and preliminary validation of *q*CP measurement in the present study, intra-staging cirrhosis with reference to these advanced systems can be our next objective in a clinical study.

To address the diverse needs in clinical practice, the development of *q*CP will carry on in two aspects. One is evaluating *q*CP performance in different clinical settings, such as the in-study cohorts of CHB or the other major etiologies. Another one is identifying the clinical relevance of *q*CP measurement, e.g. the association with response to treatment or the correlation with other key clinical markers, such as HVPG and clinical stages [1, 39], given that they are well validated in predicting the major clinical outcomes of progressive cirrhosis.



**Acknowledgements**

We thank Dr. Wei Yang (Guangdong Provincial Key Laboratory of Medical Image Processing, School of Biomedical Engineering, Southern Medical University) for his suggestion on the algorithm models for data classification and validation; and Ms.s Chu-Wen Lin and Xiao-Li Huang (School of Clinical Medicine, Zhujiang Hospital, Southern Medical University) for their assist in maintenance of the animal model. This study is partly supported by the National Natural Science Foundation of China (81371603, 81670522) and Guangdong Science and Technology Plan Project (2013B051000051) to Prof. Yan Wang; and the National Science and Technology Major Project of China (2012ZX10002003) and Guangzhou Science and Technology Plan Project (201607020019) to Prof. Jinlin Hou.

## REFERENCES


1 Tsochatzis EA, Bosch J, Burroughs AK. Liver cirrhosis. Lancet. 2014; 383: 1749-61.

2 Marcellin P, Gane E, Buti M, Afdhal N, Sievert W, Jacobson IM, et al. Regression of cirrhosis during treatment with tenofovir disoproxil fumarate for chronic hepatitis B: a 5-year open-label follow-up study. Lancet. 2013; 381: 468-75.

3 D'Ambrosio R, Aghemo A, Rumi MG, Ronchi G, Donato MF, Paradis V, et al. A morphometric and immunohistochemical study to assess the benefit of a sustained virological response in hepatitis C virus patients with cirrhosis. Hepatology. 2012; 56: 532-43.

4 Trautwein C, Friedman SL, Schuppan D, Pinzani M. Hepatic fibrosis: Concept to treatment. J Hepatol. 2015; 62: S15-24.

5 Ishak K, Baptista A, Bianchi L, Callea F, De Groote J, Gudat F, et al. Histological grading and staging of chronic hepatitis. J Hepatol. 1995; 22: 696-9.

6 Anthony PP, Ishak KG, Nayak NC, Poulsen HE, Scheuer PJ, Sobin LH. The morphology of cirrhosis. Recommendations on definition, nomenclature, and classification by a working group sponsored by the World Health Organization. J Clin Pathol. 1978; 31: 395-414.

7 Wanless IR, Sweeney G, Dhillon AP, Guido M, Piga A, Galanello R, et al. Lack of progressive hepatic fibrosis during long-term therapy with deferiprone in subjects with transfusion-dependent beta-thalassemia. Blood. 2002; 100: 1566-9.

8 Nagula S, Jain D, Groszmann RJ, Garcia-Tsao G. Histological-hemodynamic correlation in cirrhosis-a histological classification of the severity of cirrhosis. J Hepatol. 2006; 44: 111-7.

9 Kumar M, Sakhuja P, Kumar A, Manglik N, Choudhury A, Hissar S, et al. Histological subclassification of cirrhosis based on histological-haemodynamic correlation. Aliment Pharmacol Ther. 2008; 27: 771-9.

10 Germani G, Dhillon A, Andreana L, Calvaruso V, Manousou P, Isgro G, et al. Histological subclassification of cirrhosis. Hepatology. 2010; 52: 804-5.

11 Kim MY, Cho MY, Baik SK, Park HJ, Jeon HK, Im CK, et al. Histological subclassification of cirrhosis using the Laennec fibrosis scoring system correlates with clinical stage and grade of portal hypertension. J Hepatol. 2011; 55: 1004-9.

12 Tsochatzis E, Bruno S, Isgro G, Hall A, Theocharidou E, Manousou P, et al. Collagen proportionate area is superior to other histological methods for sub-classifying cirrhosis and determining prognosis. J Hepatol. 2014; 60: 948-54.

13 Calvaruso V, Burroughs AK, Standish R, Manousou P, Grillo F, Leandro G, et al. Computer-assisted image analysis of liver collagen: relationship to Ishak scoring and hepatic venous pressure gradient. Hepatology. 2009; 49: 1236-44.

14 Manousou P, Dhillon AP, Isgro G, Calvaruso V, Luong TV, Tsochatzis E, et al. Digital image analysis of liver collagen predicts clinical outcome of recurrent hepatitis C virus 1 year after liver transplantation. Liver Transpl. 2011; 17: 178-88.

15 Calvaruso V, Dhillon AP, Tsochatzis E, Manousou P, Grillo F, Germani G, et al. Liver

collagen proportionate area predicts decompensation in patients with recurrent hepatitis C virus cirrhosis after liver transplantation. J Gastroenterol Hepatol. 2012; 27: 1227-32.

16 Denk W, Strickler JH, Webb WW. Two-photon laser scanning fluorescence microscopy. Science. 1990; 248: 73-6.

17 Xu S, Wang Y, Tai DC, Wang S, Cheng CL, Peng Q, et al. qFibrosis: a fully-quantitative innovative method incorporating histological features to facilitate accurate fibrosis scoring in animal model and chronic hepatitis B patients. J Hepatol. 2014; 61: 260-9.

18 Sethasine S, Jain D, Groszmann RJ, Garcia-Tsao G. Quantitative histological-hemodynamic correlations in cirrhosis. Hepatology. 2012; 55: 1146-53.

19 Bedossa P, Garcia-Tsao G, Jain D. Cirrhosis Regression and Subclassification. Surgical Pathology Clinics. 2013; 6: 295-309.

20 Issa R, Zhou X, Constandinou CM, Fallowfield J, Millward-Sadler H, Gaca MD, et al. Spontaneous recovery from micronodular cirrhosis: evidence for incomplete resolution associated with matrix cross-linking. Gastroenterology. 2004; 126: 1795-808.

21 Heckerman D, Meek C. Models and selection criteria for regression and classification. *Proceedings of the Thirteenth conference on Uncertainty in artificial intelligence*: Morgan Kaufmann Publishers Inc. 1997:223-8.

22 Kohavi R. A study of cross-validation and bootstrap for accuracy estimation and model selection. IJCAI'95 Proceedings of the 14th international joint conference on Artificial intelligence 1995:1137-43.

23 Goodman ZD, Becker RL, Jr., Pockros PJ, Afdhal NH. Progression of fibrosis in advanced chronic hepatitis C: evaluation by morphometric image analysis. Hepatology. 2007; 45: 886-94.

24 Fontana RJ, Goodman ZD, Dienstag JL, Bonkovsky HL, Naishadham D, Sterling RK, et al. Relationship of serum fibrosis markers with liver fibrosis stage and collagen content in patients with advanced chronic hepatitis C. Hepatology. 2008; 47: 789-98.

25 Goodman ZD, Afdhal NH, Buti M, Gane EJ, Krastev Z, Schall REA, et al. Morphometric assessment of quantitative collagen and liver fibrosis in patients with chronic hepatitis B (CHB) treated for up to five years with tenofovir disoproxil fumarate (TDF). Hepatology. 2013:596A-7A.

26 Shiha G, Sarin SK, Ibrahim AE, Omata M, Kumar A, Lesmana LA, et al. Liver fibrosis: consensus recommendations of the Asian Pacific Association for the Study of the Liver (APASL). Hepatol Int. 2009; 3: 323-33.

27 Germani G, Hytiroglou P, Fotiadu A, Burroughs AK, Dhillon AP. Assessment of fibrosis and cirrhosis in liver biopsies: an update. Semin Liver Dis. 2011; 31: 82-90.

28 Runyon BA, Sugano S, Kanel G, Mellencamp MA. A rodent model of cirrhosis, ascites, and bacterial peritonitis. Gastroenterology. 1991; 100: 489-93.

29 Hui AY, Liew CT, Go MY, Chim AM, Chan HL, Leung NW, et al. Quantitative assessment of fibrosis in liver biopsies from patients with chronic hepatitis B. Liver Int. 2004; 24: 611-8.

30 Sandrini J, Boursier J, Chaigneau J, Sturm N, Zarski JP, Le Bail B, et al. Quantification of portal-bridging fibrosis area more accurately reflects fibrosis stage and liver stiffness than whole fibrosis or perisinusoidal fibrosis areas in chronic hepatitis C. Mod Pathol. 2014; 27: 1035-45.

31 Gailhouste L, Le Grand Y, Odin C, Guyader D, Turlin B, Ezan F, et al. Fibrillar collagen scoring by second harmonic microscopy: a new tool in the assessment of liver fibrosis. J Hepatol. 2010; 52: 398-406.

32 Sun TL, Liu Y, Sung MC, Chen HC, Yang CH, Hovhannisyan V, et al. Ex vivo imaging and quantification of liver fibrosis using second-harmonic generation microscopy. J Biomed Opt. 2010; 15: 036002.

33 Stanciu SG, Xu S, Peng Q, Yan J, Stanciu GA, Welsch RE, et al. Experimenting liver fibrosis diagnostic by two photon excitation microscopy and Bag-of-Features image classification. Sci Rep. 2014; 4: 4636.

34 Wang TH, Chen TC, Teng X, Liang KH, Yeh CT. Automated biphasic morphological assessment of hepatitis B-related liver fibrosis using second harmonic generation microscopy. Sci Rep. 2015; 5: 12962.

35 WHO. Hepatitis B. Fact sheet N°204. WHO Media Centre 2015.

36 Papatheodoridis GV, Dalekos GN, Yurdaydin C, Buti M, Goulis J, Arends P, et al. Incidence and predictors of hepatocellular carcinoma in Caucasian chronic hepatitis B patients receiving entecavir or tenofovir. J Hepatol. 2015; 62: 363-70.

37 Jung KS, Kim SU, Song K, Park JY, Kim DY, Ahn SH, et al. Validation of hepatitis B virus-related hepatocellular carcinoma prediction models in the era of antiviral therapy. Hepatology. 2015; 62: 1757-66.

38 Rockey DC, Caldwell SH, Goodman ZD, Nelson RC, Smith AD, American Association for the Study of Liver D. Liver biopsy. Hepatology. 2009; 49: 1017-44.

39 Ripoll C, Groszmann R, Garcia-Tsao G, Grace N, Burroughs A, Planas R, et al. Hepatic venous pressure gradient predicts clinical decompensation in patients with compensated cirrhosis. Gastroenterology. 2007; 133: 481-8.

**Table 1.** Correlations between Ishak fibrosis scores and histological cirrhosis parameters (HCPs) in the chronic hepatitis B liver biopsies.

| HCP | Spearman correlation coefficient | p value |
|---|---|---|
| Vascular area | 0.06 | 0.52 |
| Vascular perimeter | -0.01 | 0.94 |
| Vascular long-axis length | -0.02 | 0.84 |
| Vascular short-axis length | 0.05 | 0.65 |
| Vascular thickness | 0.08 | 0.44 |
| Vascular density | 0.27 | 0.006* |
| CPA | 0.83 | <0.001* |
| SPA | 0.84 | <0.001* |
| FPA | 0.36 | <0.001* |
| VPA | 0.25 | 0.01* |
| Nodule area | 0.48 | <0.001* |
| Nodule long-axis length | 0.63 | <0.001* |
| Nodule short-axis length | 0.63 | <0.001* |
| Nodule density | 0.87 | <0.001* |

*Statistically significant. CPA, total collagen proportionate area; SPA, septal collagen proportionate area; FPA, sinusoidal collagen proportionate area; VPA, vessel collagen proportionate area.

**Table 2.** Characteristics of *q*CP-index relative to Ishak fibrosis scoring in the chronic hepatitis B liver biopsies.

| Ishak stage | Biopsy number | *q*CP-index | | | | | |
|---|---|---|---|---|---|---|---|
| | | Median | Minimum | Maximum | 95%*CI* | Mean | SEM |
| F4 | 33 | 0.18 | 0.13 | 0.45 | 0.17-0.22 | 0.20 | 0.07 |
| F5 | 35 | 0.46 | 0.14 | 0.83 | 0.42-0.52 | 0.47 | 0.16 |
| F6 | 27 | 0.80 | 0.48 | 0.91 | 0.71-0.82 | 0.76 | 0.14 |

SEM, standard error of mean; CI, confidence interval.

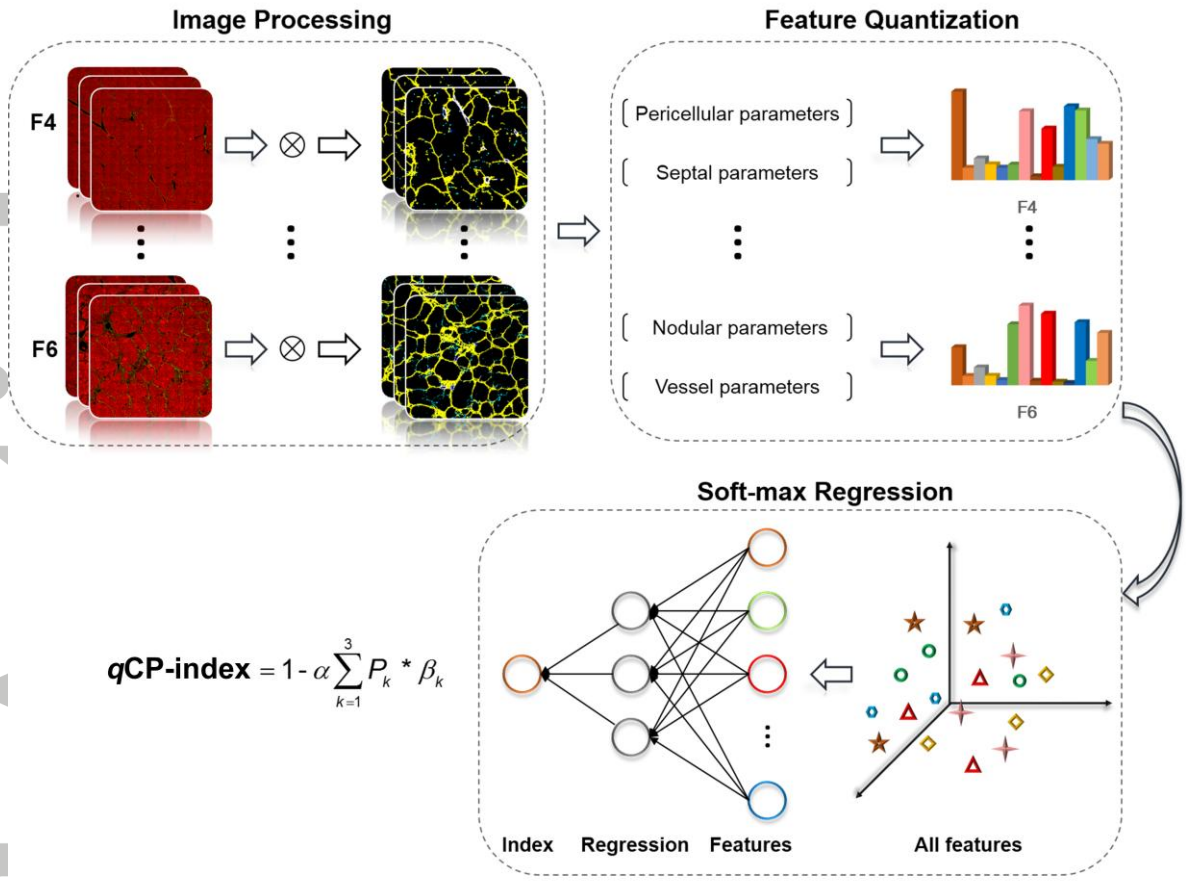


**Fig. 1. Illustration of developing an algorithm for quantitating the histological cirrhosis parameters (HCPs).** Collagen patterns were set as the elemental features of image. By image processing and feature quantitation, HCPs of these patterns were quantitatively identified. *q*CP-index was then built with the HCPs using a soft-max regression.

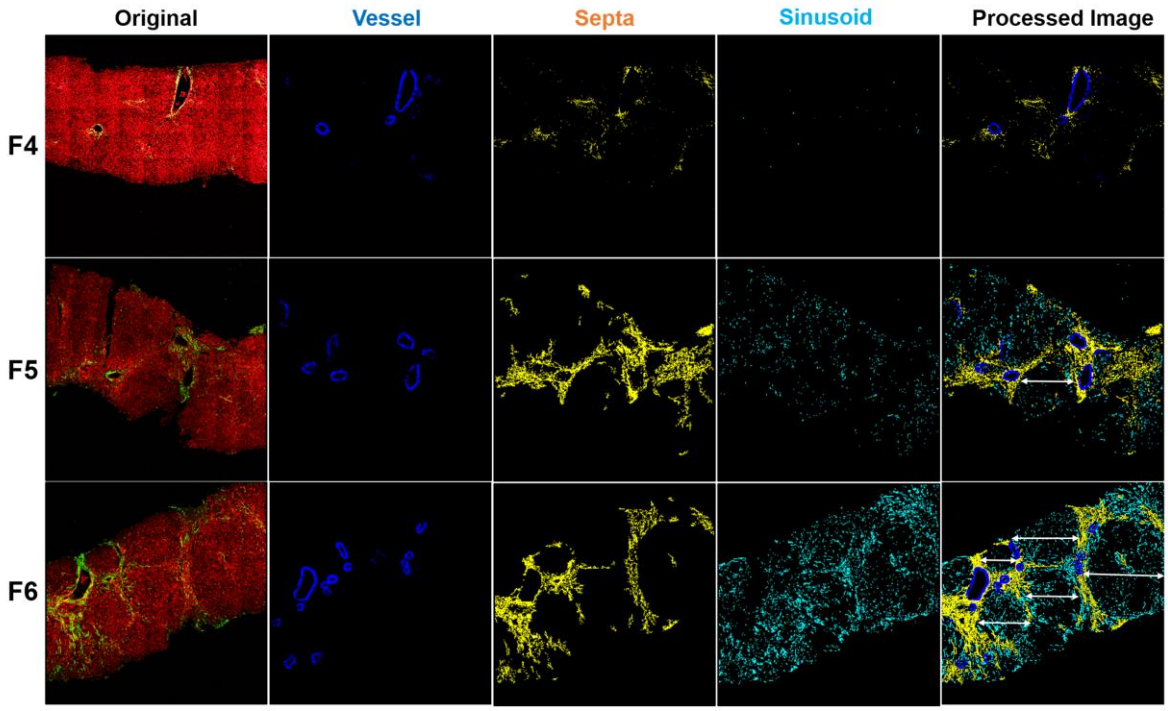


**Fig. 2. Imaging analysis of histological cirrhosis parameters in the chronic hepatitis B liver biopsies.** Raw images (green/red) for the liver biopsies at Ishak stages F4-6 and their respective processed images with principle histological patterns, including vessel (blue), septa (yellow) and sinusoid (cyan), are represented. White arrows show the cirrhotic nodules detected. Note that all the fluorescent colors were the pseudo color coded by second harmonic microscopy software which detects the endogenous signal of fibrous collagen (green) and hepatic parenchyma (red) for generating the raw images, or *q*CP which identifies the principle histological patterns in the raw images with computerized image analysis for generating the processed images.

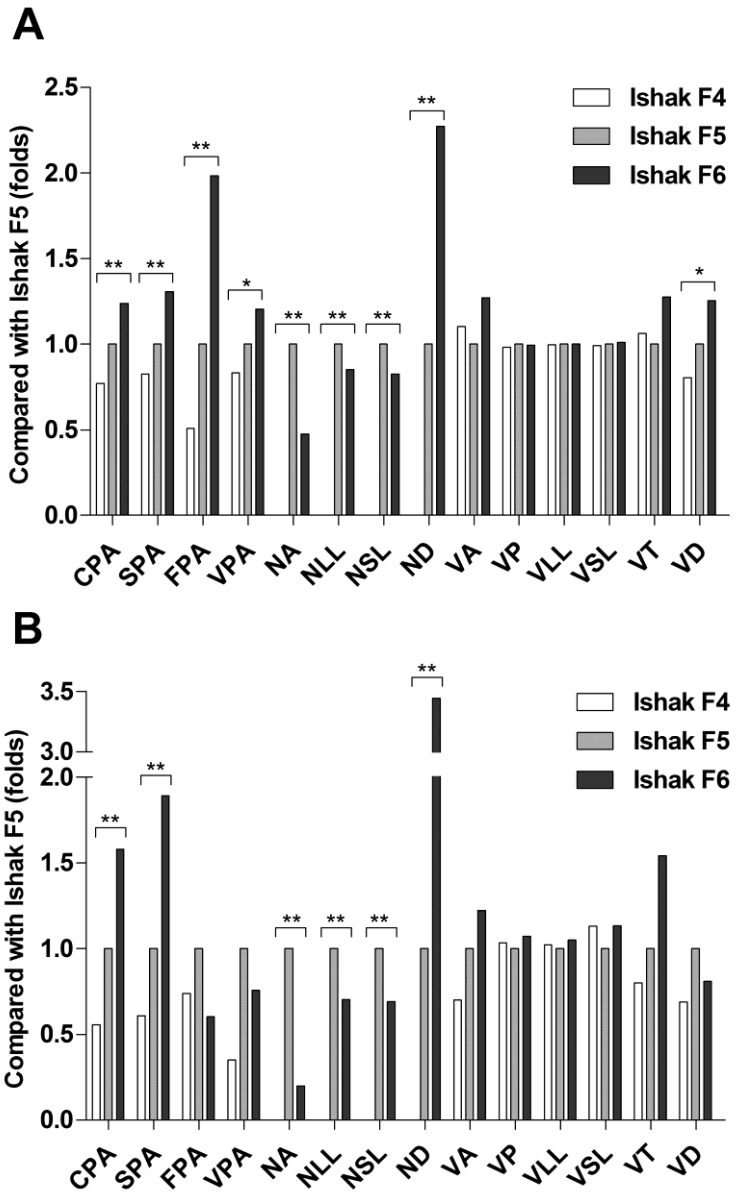


**Fig. 3. Changes in histological cirrhosis parameters (HCPs) between Ishak fibrosis stages. (A)** Chronic hepatitis B liver biopsies, **(B)** animal model. CPA, collagen proportionate area; SPA, septal collagen proportionate area; FPA, sinusoidal collagen proportionate area; VPA, vessel collagen proportionate area; NA, nodule area; NLL, nodule long-axis length; NSL, nodule short-axis length; ND, nodule density; VA, vascular area; VP, vascular perimeter; VLL, vascular long-axis length; VSL, vascular short-axis length; VT, vascular thickness; VD, vascular density. * $p<0.05$, ** $p<0.01$.

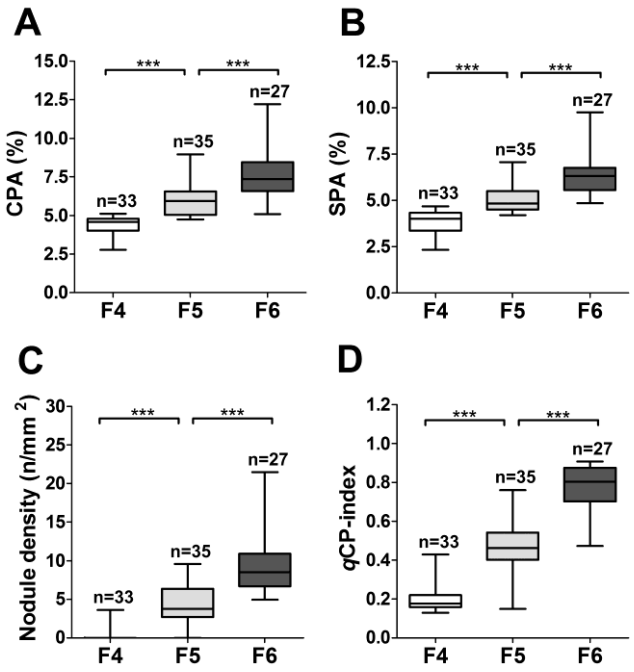


**Fig. 4. Distributions of CPA, SPA, ND and *q*CP-index at Ishak fibrosis stages in chronic hepatitis B liver biopsies. (A)** Total collagen proportionate area (CPA), **(B)** septal collagen proportionate area (SPA), **(C)** nodule density (ND), and **(D)** *q*CP-index. Box shows median, interquartile range, and minimum-maximum range. *** p<0.001.

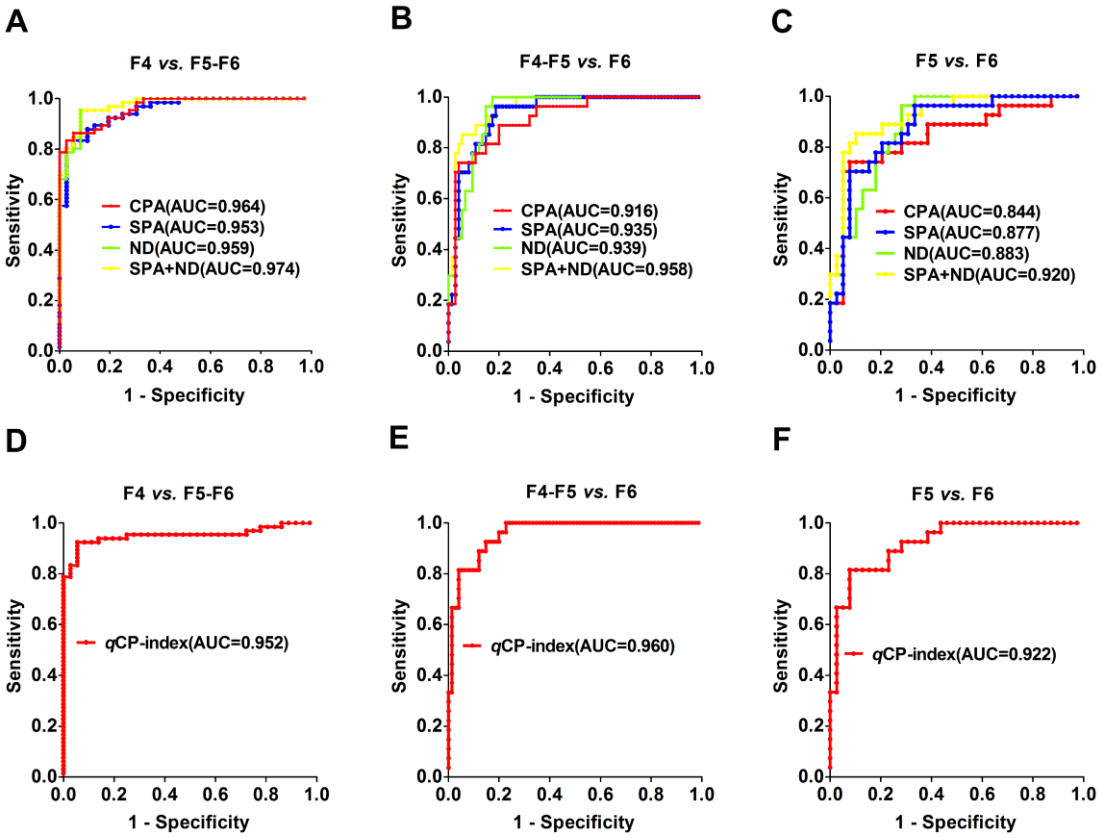


**Fig. 5. Performances of histological cirrhosis parameters (HCPs) and *q*CP-index for discriminating Ishak fibrosis stages in chronic hepatitis B liver biopsies.** HCPs: **(A)** F4 *vs.* F5-6; **(B)** F4-5 *vs.* F6; and **(C)** F5 *vs.* F6. *q*CP-index: **(D)** F4 *vs.* F5-6; **(E)** F4-5 *vs.* F6; and **(F)** F5 *vs.* F6.